1.6 W continuous-wave Raman laser using low-loss synthetic diamond

Walter Lubeigt,[1,*] Vasili G. Savitski,[1] Gerald M. Bonner,[1,2] Sarah L. Geoghegan,[3] Ian Friel,[3] Jennifer E. Hastie,[1] Martin D. Dawson,[1] David Burns,[1] and Alan J. Kemp[1]

[1]Institute of Photonics, University of Strathclyde, SUPA, 106 Rottenrow, Glasgow G4 0NW, UK
[2]MQ Photonics, Macquarie University, Sydney, NSW 2109, Australia
[3]Element Six Ltd., King's Ride Park, Ascot, SL5 8BP, UK
**walter.lubeigt@strath.ac.uk*

Abstract: Low-birefringence ($\Delta n<2x10^{-6}$), low-loss (absorption coefficient $<0.006cm^{-1}$ at 1064nm), single-crystal, synthetic diamond has been exploited in a CW Raman laser. The diamond Raman laser was intracavity pumped within a Nd:YVO_4 laser. At the Raman laser wavelength of 1240nm, CW output powers of 1.6W and a slope efficiency with respect to the absorbed diode-laser pump power (at 808nm) of ~18% were measured. In quasi-CW operation, maximum on-time output powers of 2.8W (slope efficiency ~24%) were observed, resulting in an absorbed diode-laser pump power to the Raman laser output power conversion efficiency of 13%.

OCIS codes: (140.3580) Laser, solid-state; (140.3550) Laser, Raman; (160.4670) Optical materials.

References and links

1. P. Cerný, H. Jelinkova, P. G. Zverev, and T. T. Basiev, "Solid state lasers with Raman frequency conversion," Prog. Quantum Electron. **28**(2), 113–143 (2004).
2. J. Piper and H. Pask, "Crystalline Raman lasers," IEEE J. Sel. Top. Quantum Electron. **13**(3), 692–704 (2007).
3. R. P. Mildren and A. Sabella, "Highly efficient diamond Raman laser," Opt. Lett. **34**(18), 2811–2813 (2009).
4. D. J. Spence, E. Granados, and R. P. Mildren, "Mode-locked picosecond diamond Raman laser," Opt. Lett. **35**(4), 556–558 (2010).
5. A. Sabella, J. A. Piper, and R. P. Mildren, "1240 nm diamond Raman laser operating near the quantum limit," Opt. Lett. **35**(23), 3874–3876 (2010).
6. J. P. M. Feve, K. E. Shortoff, M. J. Bohn, and J. K. Brasseur, "High average power diamond Raman laser," Opt. Express **19**(2), 913–922 (2011).
7. A. A. Demidovich, A. S. Grabtchikov, V. A. Orlovich, M. B. Danailov, and W. Kiefer, "Diode pumped diamond Raman microchip laser," in *2005 Conference on Lasers and Electro-Optics Europe*, (Munich, 2005), p. 251.
8. W. Lubeigt, G. M. Bonner, J. E. Hastie, M. D. Dawson, D. Burns, and A. J. Kemp, "An intra-cavity Raman laser using synthetic single-crystal diamond," Opt. Express **18**(16), 16765–16770 (2010).
9. W. Lubeigt, G. M. Bonner, J. E. Hastie, M. D. Dawson, D. Burns, and A. J. Kemp, "Continuous-wave diamond Raman laser," Opt. Lett. **35**(17), 2994–2996 (2010).
10. P. M. Martineau, M. P. Gaukroger, K. B. Guy, S. C. Lawson, D. J. Twitchen, I. Friel, J. O. Hansen, G. C. Summerton, T. P. G. Addison, and R. Burns, "High crystalline quality single crystal chemical vapour deposition diamond," J. Phys. Condens. Matter **21**(36), 364205 (2009).
11. R. S. Balmer, J. R. Brandon, S. L. Clewes, H. K. Dhillon, J. M. Dodson, I. Friel, P. N. Inglis, T. D. Madgwick, M. L. Markham, T. P. Mollart, N. Perkins, G. A. Scarsbrook, D. J. Twitchen, A. J. Whitehead, J. J. Wilman, and S. M. Woollard, "Chemical vapour deposition synthetic diamond: materials, technology and applications," J. Phys. Condens. Matter **21**(36), 364221 (2009).
12. H. Jelinkova, O. Kitzler, V. Kubecek, M. Jelinek, M. Cech, J. Sulc, and M. Nemec, "Single pass SRS threshold and gain from diamond under 532nm picoseconds Nd:YAG pulse pumping," WeP14, Europhoton 2010, European Physical Society, Mulhouse, France (2010).
13. A. A. Kaminskii, R. J. Hemley, J. Lai, C. S. Yan, H. K. Mao, V. G. Ralchenko, H. J. Eichler, and H. Rhee, "High-order stimulated Raman scattering in CVD single crystal diamond," Laser Phys. Lett. **4**(5), 350–353 (2007).
14. A. A. Kaminskii, V. G. Ralchenko, and V. I. Konov, "CVD-diamond – a novel $\chi(3)$-nonlinear active crystalline material for SRS generation in very wide spectral range," Laser Phys. Lett. **3**(4), 171–177 (2006).
15. H. Herchen and M. A. Cappelli, "First-order Raman spectrum of diamond at high temperatures," Phys. Rev. B Condens. Matter **43**(14), 11740–11744 (1991).
16. D. Nikogosyan, *Handbook of Properties of Optical Materials* (John Wiley and Sons Ltd., 1997).

#141464 - $15.00 USD Received 20 Jan 2011; revised 11 Mar 2011; accepted 13 Mar 2011; published 25 Mar 2011

17. P. Millar, R. B. Birch, A. J. Kemp, and D. Burns, "Synthetic diamond for intracavity thermal management in compact solid-state lasers," IEEE J. Quantum Electron. **44**(8), 709–717 (2008).
18. I. Friel, S. L. Clewes, H. K. Dhillon, N. Perkins, D. J. Twitchen, and G. A. Scarsbrook, "Control of surface and bulk crystalline quality in single crystal diamond grown by chemical vapour deposition," Diamond Related Materials **18**(5-8), 808–815 (2009).
19. A. M. Glazer, J. G. Lewis, and W. Kaminsky, "An automatic optical imaging system for birefringent media," Proc. R. Soc. Lond. A **452**(1955), 2751–2765 (1996).
20. P. M. Martineau, S. C. Lawson, A. J. Taylor, S. J. Quinn, D. J. F. Evans, and M. J. Crowder, "Identification of synthetic diamond grown using chemical vapor deposition," Gems Gemol. **40**, 2–25 (2004).
21. M. E. Newton, "Neutral and ionized single substitutional nitrogen in diamond," in *Properties, Growth and Applications of Diamond*, M. H. Nazare and A. J. T. Neves, eds., (Institution of Engineering and Technology, 2001).
22. ISO 11551:2003, "Test method for absorptance of optical laser components."
23. G. Turri, Y. Chen, M. Bass, D. Orchard, J. E. Butler, S. Magana, T. Feygelson, D. Thiel, K. Fourspring, R. V. Dewees, J. M. Bennett, J. Pentony, S. Hawkins, M. Baronowski, A. Guenthner, M. D. Seltzer, D. C. Harris, and C. M. Stickley, "Optical absorption, depolarization, and scatter of epitaxial single-crystal chemical-vapor deposited diamond at 1.064um," Opt. Eng. **46**(6), 064002 (2007).
24. Z. L. Liau, "Semiconductor wafer bonding via liquid capillarity," Appl. Phys. Lett. **77**(5), 651–653 (2000).
25. M. E. Innocenzi, H. T. Yura, C. L. Fincher, and R. A. Fields, "Thermal modeling of continuous-wave end-pumped solid-state lasers," Appl. Phys. Lett. **56**(19), 1831–1833 (1990).

1. Introduction

Crystalline Raman lasers enable wavelengths between 1.1 and 1.6μm to be reached using systems based on ubiquitous neodymium lasers [1,2]. Recently, the use of high optical quality, single-crystal, synthetic diamond as a Raman material in external cavity [3–6] and intracavity [7–9] configurations has been demonstrated – made possible by the progress in diamond chemical vapour deposition (CVD) [10,11]. Diamond has a large Raman gain (64cm/GW at λ = 532nm [12] and between 12.5cm/GW [13] and 16.6cm/GW [5] at λ = 1064nm), broad transparency (0.23-2.5μm and >7μm [14]) and a large Raman shift (1332cm^{-1} [15]). Its thermal conductivity (2000W/m.K [16]) is 2 to 3 orders of magnitude greater than typical crystalline Raman media such as $KGd(WO_4)_2$ and YVO_4 – reducing thermal lensing and hence increasing the power scaling potential of continuous-wave (CW) Raman lasers [2]. In this paper, the use of CVD-grown, low-loss, low-birefringence diamond as a Raman medium in a CW Nd:YVO_4 disk laser is reported. By improving the thermal management of the pump laser gain medium (Nd:YVO_4) using a diamond heat spreader [17], and using a lower loss diamond as the Raman laser medium, CW output powers of 1.6W at the Raman laser wavelength (1240nm) were achieved, eight times higher than previously reported [9]. The next section describes the diamond sample. Section 3 outlines the laser architecture; the results are outlined and discussed in sections 4 and 5.

2. Diamond Raman laser configuration

2.1 Low-loss synthetic diamond

The Raman laser medium was a 4.1mm long, single-crystal, CVD diamond plate with a 3.1mm × 1.6mm cross-section. The 1.6, 3.1 and 4.1mm edges were parallel to <100>, <110>, and <110> directions respectively. The sample was grown homoepitaxially by microwave-plasma chemical vapour deposition on a {100} type Ib synthetic diamond substrate in a $H_2/CH_4/N_2$ gas atmosphere. The substrate was carefully prepared to minimize surface and sub–surface damage in order to reduce the dislocation density commensurate with low birefringence material [18]. After growth, the CVD diamond layer was removed from the substrate by laser sawing and polished to provide a high optical quality finish. Birefringence, Δn, along <110> – the direction of light propagation in the Raman laser experiments – was measured to be between 9×10^{-7} and 2×10^{-6} using the Metripol technique [19]. Optical absorption in synthetic diamond is broadly determined by levels of nitrogen-containing defects (ignoring the 2.5-6μm multiphonon absorption band), the most important being single substitutional nitrogen – a nitrogen atom substituted for a carbon atom on the diamond lattice. This defect gives rise to absorption features in the UV, visible and infrared spectral ranges [20]. The level of nitrogen was estimated using electron paramagnetic resonance (EPR)

#141464 - $15.00 USD Received 20 Jan 2011; revised 11 Mar 2011; accepted 13 Mar 2011; published 25 Mar 2011

measurements [21] taken on other representative samples. This determines the density of single substitutional nitrogen in its neutral charge state (N_S^0) only. However, this is the dominant nitrogen–containing impurity, and the density was estimated to be 20 ± 10 ppb. The absorption coefficient at 1064nm was measured to be <0.001cm^{-1} by Laser Zentrum Hannover e.V., using ISO-standard calorimetry [22]. Anti-reflection (AR) coatings (R<0.1% at λ = 1064nm and λ = 1240nm) were then applied to the front and back surfaces. The absorption coefficient was then measured to be <0.006cm^{-1} using a simplified calorimetry technique similar to that in [3], rather than the ISO approved methodology. The diamond sample was mounted in a thermo-electrically cooled brass mount. With a 1064nm beam passing through the sample, the current required to maintain a constant sample temperature was recorded and calibrated against a known heat load provided by a precision resistor. The higher upper bound given by this technique compared to the ISO approach results from its lower accuracy, the effect of the coatings (these had some visible damage as a result of the laser experiments which may have contributed to the measured absorption), and the effect of any scattered light absorbed in the mount. Even so, an absorption coefficient of <0.006cm^{-1} is a significant improvement on the sample used in [8,9] where an absorption coefficient of ~0.03cm^{-1} was measured using the same apparatus. However, laser calorimetry is not, in general, sensitive to scatter, which may be a significant fraction of the overall loss if the absorption is small [23]: a different measurement technique would be required to determine this and hence the total loss.

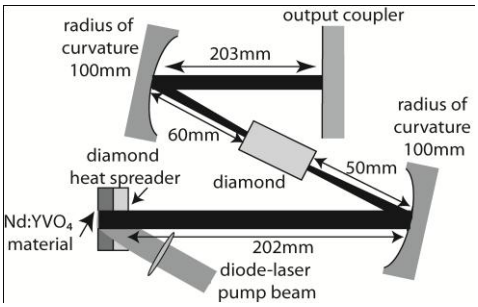

Fig. 1. Schematic of the CW diamond Raman laser.

2.2 Intracavity diamond Raman laser

A 4-mirror intracavity-pumped Raman laser resonator (Fig. 1) was built around an a-cut Nd:YVO_4 crystal (0.5mm thick, 1 atm.% doping). The rear face of the Nd:YVO_4 was high-reflectivity (HR) coated for 1064 and 1240nm (reflectivity R>99.9%), and for 808nm (R>95%). A low birefringence ($\Delta n < 3 \times 10^{-6}$), 0.5mm-thick synthetic single-crystal diamond heat spreader (4mm diameter) was bonded to the uncoated face of the Nd:YVO_4 using liquid-assisted optical contacting [24]. The other face of the diamond disk was AR coated for λ = 808 (R<10%), 1064 and 1240nm (R<0.1%). The Nd:YVO_4 / diamond structure was mounted on a water-cooled brass heat sink (water temperature = 20°C) using indium and was pumped with a 35W fibre-coupled diode-laser (100μm core diameter, 0.22 NA, λ = 808nm). The diode-laser pump spot radius in the Nd:YVO_4 crystal was 330 μm. Both curved cavity mirrors were HR coated for 1064nm and 1240nm, while the output coupler was HR coated at 1064nm and had a transmission of 1% at 1240nm. The cuboid of diamond used as the Raman laser medium was orientated for light propagation along its 4.1mm length and with the 1.6 and 3.1mm edges at 45° to the horizontal. Both the 1064 and 1240nm fields were horizontally polarized. The fundamental transverse mode radii for the pump radiation (λ = 1064nm) within the diamond and the Nd:YVO_4 were calculated to be ~60μm and ~260μm respectively.

#141464 - $15.00 USD Received 20 Jan 2011; revised 11 Mar 2011; accepted 13 Mar 2011; published 25 Mar 2011

3. Results

In this configuration, the slope efficiency of the Raman laser (λ = 1240nm) was measured to be ~18% with respect to the absorbed diode-laser pump power (Fig. 2). The maximum output power was 1.6W for an absorbed diode-laser pump power of 15W: an absorbed pump power to Raman laser conversion efficiency of ~11%. Output power stability traces are shown in Fig. 3(a) and Fig. 3(b) and demonstrate an output power variation of less than 10% over 20s. The beam propagation factors were M^2_x = 2.8 and M^2_y = 2.6 for the Raman laser (1240nm) and M^2_x = 3.4 and M^2_y = 3.5 for the pump laser (1064nm). Both lasers were horizontally polarized.

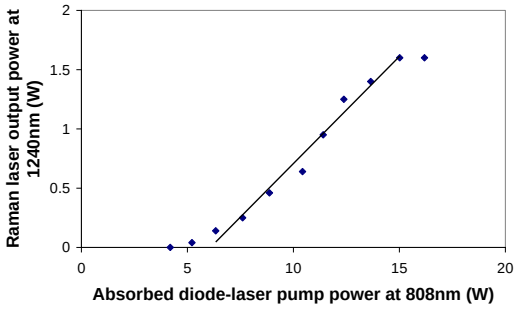

Fig. 2. Power transfer characteristic for the CW Raman laser.

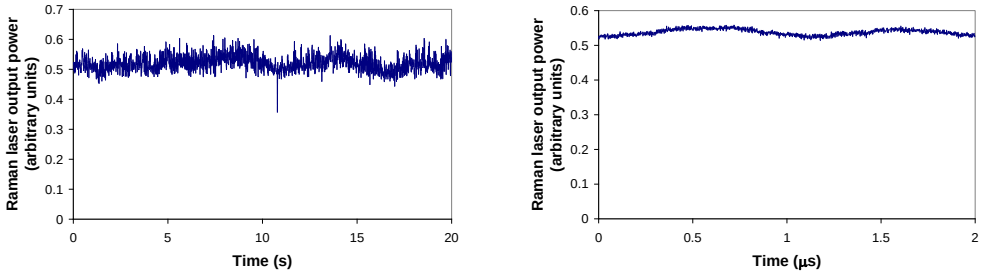

Fig. 3. (a) Longer term and (b) shorter term output power stability traces at the maximum output power (P = 1.6W) for the Raman laser. [N.B. The spike in (a) probably corresponds to a thermally-induced transverse mode change in the pump laser].

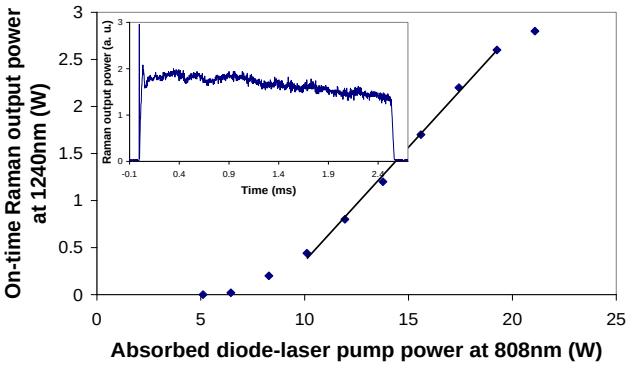

Fig. 4. On-time power transfer of the quasi-CW Raman laser and temporal dependence of the output power at the maximum pump power (inset).

#141464 - $15.00 USD Received 20 Jan 2011; revised 11 Mar 2011; accepted 13 Mar 2011; published 25 Mar 2011

The laser was operated in quasi-CW mode to assess the performance unimpeded by thermal lensing in the Nd:YVO_4. The diode-laser was chopped at a 50% duty cycle (2.5ms on/2.5ms off) giving a maximum on-time output power of 2.8W, an on-time slope efficiency of ~24% and an absorbed diode-laser pump power to Raman laser conversion efficiency of 13% (Fig. 4). Thermal effects begin to restrict the output power at the end of the pump pulse (Fig. 4, inset); however, the main limitation was the available diode-laser pump power.

4. Discussion

The output power of the CW diamond Raman laser reported here is 8 times greater than the first such laser reported in [9]. In addition, the diode-laser pump power range over which the laser oscillates is significantly increased and amplitude noise reduced. These improvements can mainly be explained by the use of a significantly lower loss diamond and improved thermal management in the laser gain medium. In the Raman laser described in [9], the large diamond-induced losses (~2% per round trip) meant that all other losses had to be minimized to enable Raman laser oscillation. A 2-mirror cavity was therefore used to reduce the component count and hence the loss. However, to ensure a small mode radius in the diamond, and hence a small Raman laser threshold, the fundamental mode radius of the pump laser (λ = 1064nm) at the centre of the Nd:YVO_4 crystal was less than half the diode-laser pump mode radius. This configuration encouraged the oscillation of higher-order transverse modes and was close to a cavity stability edge and hence extremely sensitive to thermal lensing – severely limiting the performance of the Raman laser. In contrast, for the laser described here, a lower loss diamond sample enables the use of a 4-mirror resonator where the laser mode radii in the conventional and Raman laser gain materials can be independently controlled.

The use of a diamond heat spreader reduces the thermal lensing in the Nd:YVO_4 crystal: the other factor limiting the output power achieved in [9]. This is illustrated in Fig. 5 where a simplified finite element model has been used to simulate the temperature rise at the diode-laser pump power required for maximum Raman laser output power: for the conventional Nd:YVO_4 laser rod used in [9] (Fig. 5(a)) and for the Nd:YVO_4 / diamond composite used in this work (Fig. 5(b)). (To keep the required computing resources reasonable, averaged values have been used for some anisotropic materials parameters to permit an axisymmetric simulation.) The absorbed diode-laser pump power density is higher in the present work, due to the thin piece of Nd:YVO_4 used and the higher absorbed pump power (15W as opposed to 10W) – despite a larger pump spot radius (330µm as opposed to 150µm). However, the predicted maximum temperature rise is similar in the two scenarios: 152K as opposed to 139K. As a result, the thermal lens caused by the change of refractive index with temperature is significantly weaker in the present case where a thin piece of gain material is used: a focal length of approximately 450mm as opposed to 60mm (estimated from a quadratic fit to the radial variation in the axially averaged temperature [25]). The radius of curvature of the most significant mechanical deformation was also calculated to be longer: 590mm for the HR coated surface of the Nd:YVO_4 / diamond composite in the current case as opposed to 210mm for the pumped end of the Nd:YVO_4 rod in [9]. Weaker thermal lensing means that higher diode-laser pump powers can be used without the risk of resonator instability. For the work described in this paper, roll-over of the Raman laser output power was observed for diode-laser pump powers above 15W for CW operation; such behavior was not observed in the quasi-CW experiment indicating that this effect results from thermal issues within the Nd:YVO_4. Improved thermal management in the laser gain medium, for example through the use of ytterbium-doped materials should allow for further power scaling. Therefore, diamond has the potential to compete with more conventional Raman laser (e.g. $KGd(WO_4)_2$ and YVO_4) materials in the CW regime as already demonstrated in the pulsed regime [3,5].

The use of diamond also reduces the thermal lensing in the Raman material compared to a more conventional Raman laser material such as YVO_4. This is illustrated in Fig. 6 where the thermal lens in a 4mm long diamond sample (Fig. 6(a)) is compared, theoretically, to the use of a 25mm long YVO_4 sample (Fig. 6(b)). A larger mode radius (160µm) is assumed in YVO_4 than the diamond (100µm) to reduce the thermal effects whilst maintaining a similar Raman

#141464 - $15.00 USD Received 20 Jan 2011; revised 11 Mar 2011; accepted 13 Mar 2011; published 25 Mar 2011

laser threshold. Assuming the same Raman laser output power (1.6W as per the experimental result described in section 3), the temperature rise is six-fold higher in YVO_4 and the thermal lens focal length is 30 fold shorter (0.5m as opposed to 16m). This illustrates the potential of diamond for power-scaling of CW Raman lasers. Further, so-called 'beam clean-up', leading to an improvement in the beam quality of the Raman laser over the pump laser [2], is observed in our laser indicating the potential for efficient, high brightness Raman lasers even when the beam quality of the pump laser is not perfect.

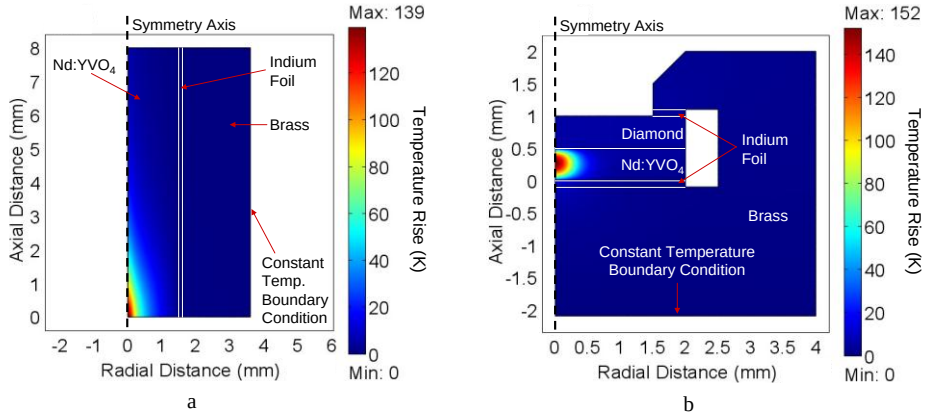

Fig. 5. Approximate simulations of the temperature rise in (a) the Nd:YVO_4 rod used in [9] and (b) the Nd:YVO_4 disk with a diamond heat spreader used in this work (cylindrical symmetry is assumed in both cases to simplify calculations).

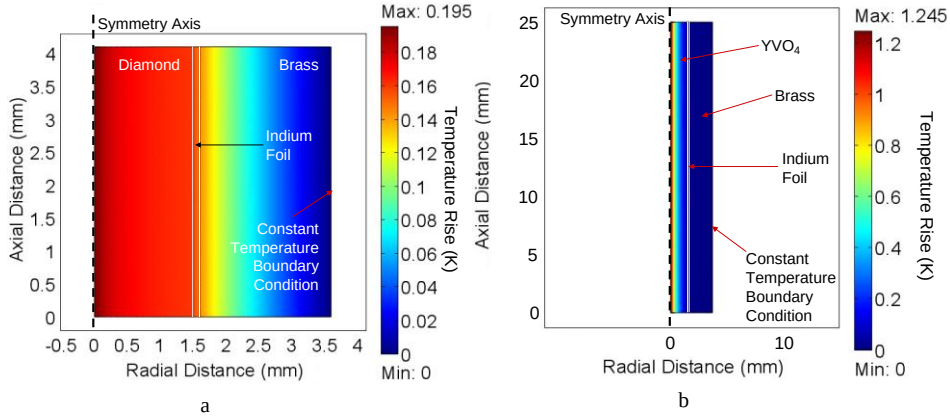

Fig. 6. Approximate simulations of the temperature rise in (a) a 4mm diamond Raman gain medium and (b) a 25mm YVO_4 Raman gain medium (cylindrical symmetry is assumed in both cases to simplify calculations).

5. Conclusion

A CW diamond Raman laser has been operated above the Watt level. The maximum output power was 1.6W and the conversion efficiency was 11% from the diode-laser pump power. In part, this was enabled by the excellent optical properties of the single-crystal synthetic diamond sample: in particular, low birefringence and low loss. In addition, thermal effects within the conventional laser gain medium were significantly reduced using a diamond heat spreader. These improvements combined to give an eight-fold increase in output power over our previous report of a CW diamond Raman laser [9].

#141464 - $15.00 USD Received 20 Jan 2011; revised 11 Mar 2011; accepted 13 Mar 2011; published 25 Mar 2011

Acknowledgments

Gerald Bonner acknowledges guidance from Helen Pask and Richard Mildren of Macquarie University. This work was supported by the UK EPSRC under grant EP/G00014X/1.

#141464 - $15.00 USD Received 20 Jan 2011; revised 11 Mar 2011; accepted 13 Mar 2011; published 25 Mar 2011